# Superfluidity of $^4$He in nanosize channels

Hiroki Ikegami*
*Low Temperature Physics Laboratory, RIKEN, Hirosawa 2-1, Wako, Saitama 351-0198, Japan*

Yoji Yamato and Tomohisa Okuno
*Graduate School of Arts and Sciences, University of Tokyo, Komaba 3-8-1, Meguro-ku, Tokyo 153-8902, Japan*

Junko Taniguchi
*Department of Applied Physics and Chemistry, University of Electrocommunication, Chofugaoka 1-5-1, Chofu, Tokyo 182-8585, Japan*

Nobuo Wada
*Department of Physics, Faculty of Science, Nagoya University, Chikusa-ku, Nagoya 464-8602, Japan*

Shinji Inagaki and Yoshiaki Fukushima
*Toyota Central R&D Laboratories, Inc., Yokomichi, Nagakute, Aichi 480-1192, Japan*
(Received 14 September 2006; revised manuscript received 29 August 2007; published 5 October 2007)

Superfluid properties of $^4$He adsorbed in nanometer-size channels have been studied using torsional oscillators for several channel diameters ranging from 1.5 to 4.7 nm. Clear evidence that $^4$He exhibits superfluidity in channels larger than 1.8 nm is obtained. The superfluid transition in channels larger than 2.8 nm is well understood in terms of the finite-size Kosterlitz-Thouless transition, where the vortex unbinding mechanism plays an essential role. This vortex mechanism, however, should break down for channels narrower than the vortex core size ($2.5 \pm 1.2$ nm). Indeed, features that are not expected on the basis of the finite-size Kosterlitz-Thouless theory are observed for channels smaller than 2.2 nm: strong suppression of the observed superfluid density and disappearance of the dissipation peak associated with the diffusive motion of the vortices.

DOI: 10.1103/PhysRevB.76.144503 PACS number(s): 67.70.+n, 67.40.−w, 67.40.Db

## I. INTRODUCTION

The dimension of a system has a significant influence on the phase coherence of the ordered state. In a low-dimensional Bose-Einstein condensate, phase fluctuation of the order parameter destroys the long-range order. In a one-dimensional (1D) system, condensation never occurs, whereas a two-dimensional (2D) condensate can exist only at zero temperature. In the 2D system, however, the Kosterlitz-Thouless (KT) mechanism drives the system into a quasicondensate state at a nonzero transition temperature, where the superfluidity is destroyed by the unbinding of vortex pairs.[1] A beautiful KT transition is demonstrated by a 2D $^4$He film adsorbed on a planar substrate.[2] For a 1D $^4$He system, however, little has been experimentally explored because of the difficulty in realizing the system.

The realization of 1D liquid $^4$He is challenging. It would be realized by $^4$He atoms being adsorbed in a cylindrical channel with diameter $d$ below a few nanometers. Because the azimuthal motion has discrete energy levels, only excitations parallel to the channel axis are allowed at low temperatures, leading to 1D behavior. Such physical systems were recently investigated using nanometer-size porous materials.[3–9] In the 1.8-nm-diameter channel, the observed heat capacity of the second layer of the $^4$He film is proportional to temperature below 0.3 K (Refs. 3 and 10); this is attributed to the 1D phonon propagating along the channel axis.

In the 2D $^4$He film, the phase coherence is maintained at low temperatures by bound vortex pairs. With increasing temperature, the vortex pairs with infinite separation are unbound at the KT transition temperature, and these unbound vortices destroy the phase coherence. In the cylindrical geometry, the finite length in the azimuthal direction affects the superfluid properties. There, the superfluid transition is understood in terms of the finite-size KT transition with the system size of $\pi d/2$,[11–14] where the phase coherence is also destroyed by the unbound vortices. This finite-size KT transition well explains the superfluid properties observed in porous glass with $d$ larger than 5 nm.[15] This mechanism, however, breaks down when $d$ becomes comparable to the vortex core diameter $a_0$, which is experimentally estimated to be $2.5 \pm 1.2$ nm.[15] A crossover from the 2D to the 1D behavior is expected at $d \sim a_0$. Studies with $d$ varied in the range of $a_0$ provide important information about the 1D Bose system.

In this paper, we present the results of the first systematic study of superfluid $^4$He adsorbed in several channels with diameter ranging from 1.5 to 4.7 nm, using torsional oscillators. We found that the superfluid transition in channels larger than 2.8 nm is explained by the finite-size KT transition, while this mechanism breaks down for channels narrower than the vortex core diameter. To obtain these conclusions, we had to overcome a technical difficulty in the use of the torsional oscillator; the oscillator detects the superfluid signal from both $^4$He in the channel and the $^4$He film coating the outer surface of the substrate grain, and therefore it is difficult to judge whether $^4$He becomes superfluid in the channel. We performed the oscillator experiments for two cases: $^4$He adsorbed (i) on bare substrates and (ii) on substrates with channels that are completely filled with $N_2$ atoms. In the latter case, the superfluid signal comes only from

 ©2007 The American Physical Society

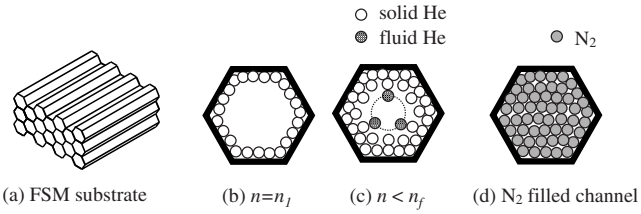


FIG. 1. (a) Schematic drawing of the FSM substrate. (b) Completion of the first layer at $n_1$. (c) The fluid layer formed on the solid helium film. (d) The channel filled with $N_2$ atoms.

the film coating the grain surface. By comparing these two cases, we could clearly see the existence of the superfluid in the channel.

## II. EXPERIMENT

To enable a clear discussion of the diameter dependence of superfluid properties, the substrate should have the following properties: uniform diameter, precise controllability of the diameter, and large surface area. Folded sheet mesoporous materials (FSM) [Fig. 1(a)] possess such properties.[16,17] They are a family of highly ordered mesoporous silica crystals with a regular arrangement of uniform hexagonal channels. The diameter can be controlled precisely from 1 to 5 nm by using alkyltrimethylammonium $[C_mH_{2m+1}N^+(CH_3)_3]$ of different alkylchain lengths in the synthesizing process of this material.

In this work, we use five varieties of FSM with diameters of 1.5, 1.8, 2.2, 2.8, and 4.7 nm. The four smaller channels correspond to the alkylchain lengths of $m=8$, 10, 14, and 16, respectively, and the 4.7 nm channel is enlarged from that of $m=16$ by adding mesitylene.[18] These substrates are in powder form with a particle size of about 0.3 $\mu$m. Therefore, the typical length of the channel is 0.3 $\mu$m. Each powder is mixed with 60 $\mu$m silver powder in a 2:1 weight ratio, pressed onto a cell of a torsional oscillator to achieve good thermal contact, and then dehydrated in vacuum at 170 °C. Surface areas are determined by the Brunauer-Emmett-Teller (BET) fitting of a $N_2$ adsorption isotherm at 77 K with an area of a nitrogen molecule of 16.2 Å$^2$/atom. The surface areas are summarized in Table I. In the table, the pressure range for the fitting is also included. The area of the outer surface of the FSM grains, as estimated from the powder size, is about 1% of the total surface area.

To study the properties of the superfluid film formed in those channels, we employed torsional oscillators, the most powerful technique for the study of superfluid properties. Some important parameters of the torsional oscillators are summarized in Table I. The resonant frequency $F$ of each torsional oscillator is around 1100 kHz. The quality factor $Q$ is of the order of $10^6$ because of the use of aluminum alloy 5056 as a torsion rod. A shift of the resonant frequency $\Delta F$ and a change in the inverse of the quality factor $\Delta Q^{-1}$ are observed when the helium film becomes superfluid. $\Delta F$ is proportional to the amount of helium film that decouples from the substrate motion and $\Delta Q^{-1}$ is proportional to the energy dissipated in the film.

The tortuosity factor $\chi$ of the oscillator is defined by $\chi = (|\partial F/\partial n|_s)/(|\partial F/\partial n|_n)$, where $|\partial F/\partial n|_n$ and $|\partial F/\partial n|_s$ are the mass sensitivity of the oscillator at zero temperature in the coverage region of $n < n_{on}$ and $n > n_{on}$, respectively. Here, $n$ is the coverage of the helium film and $n_{on}$ is the superfluid onset coverage. $1-\chi$, which reflects the fraction of the superfluid that decouples from the substrate motion, is about 0.05–0.1 except in the case of the 1.5 nm channel (Table I). For the 1.5 nm channel, $1-\chi$ is about twice larger than for the other cases. It should be noted that, for the 1.5 nm channel, the superfluid signal comes not from $^4$He in the channel but from the film coating the FSM grain surface, as discussed in Sec. V A.

The torsional oscillators are mounted on a mixing chamber of a dilution refrigerator. $^4$He sample is introduced and annealed at around 4.2 K to ensure a film with a uniform thickness.

When preparing the channels filled with $N_2$ atoms, $N_2$ gas is admitted into the cell at 77 K up to the vapor pressure of 90 kPa. At this pressure, the channels are completely filled with $N_2$ atoms. Then, the refrigerator is slowly cooled to 67 K to reduce the vapor pressure of $N_2$ in the filling line and hence avoid plugging the line. After that, it is cooled slowly to 4.2 K.

TABLE I. Important parameters of the FSM substrates and the torsional oscillators (see text).

| Diameter | 1.5 nm | 1.8 nm | 2.2 nm | 2.8 nm | 4.7 nm |
|---|---|---|---|---|---|
| | | FSM substrate | | | |
| Amount of FSM (g) | 0.363 | 0.250 | 0.207 | 0.181 | 0.201 |
| Surface area (m$^2$) | 195 | 157 | 178 | 182 | 135 |
| BET fitting range (kPa) | 2–15 | 5–15 | 5–15 | 5–22 | 5–22 |
| $n_1$ (mmol) | | 2.16 | 2.97 | 3.20 | 2.38 |
| | | Torsional oscillator | | | |
| Resonant frequency (Hz) | 1159 | 1131 | 1136 | 1115 | 1106 |
| $\lvert\partial F/\partial n\rvert_n$ (Hz/mmol) | 0.1763 | 0.1648 | 0.1775 | 0.1735 | 0.1716 |
| $\lvert\partial F/\partial n\rvert_s$ (Hz/mmol) | 0.1441 | 0.1508 | 0.1692 | 0.1569 | 0.1592 |
| $1-\chi$ | 0.18 | 0.085 | 0.047 | 0.096 | 0.072 |

## III. FILM GROWTH IN CHANNELS OF FOLDED SHEET MESOPOROUS MATERIALS

The growth of the helium film in the FSM channel is now understood as a result of our accurate vapor pressure[19] and heat capacity measurements.[3,20] $^4$He atoms introduced into a cell are adsorbed into the channels and onto the outer surface of the substrate grains in amounts proportional to the ratio of their surface areas. In the channel, the adsorbed film forms a cylindrical tube on the wall of the channel. The first layer is completed with monolayer coverage $n_1$ [Fig. 1(b)], and then the second layer is formed on top of the first layer. The film is solid until slightly above $n_1$, after which a fluid phase appears on the solid film [Fig. 1(c)]. The coverage at which the fluid phase appears depends on the channel diameter and is between $n_1$ and $2n_1$, typically $1.15n_1$ and $1.4n_1$ for the 1.8 and 2.8 nm channels, respectively.[3,20] The very thin fluid film formed on the solid film is not superfluid. In this paper, we call the combination of the solid film and the very thin normal fluid film an inert film. With further increase of $n$, the adsorbed film becomes superfluid and grows uniformly up to full pore coverage $n_f$ without capillary condensation. Above $n_f$, the introduced helium atoms are mainly adsorbed onto the outer surface of the grain, causing a rapid increase in the thickness of the film there. Above $n_f$, however, a fraction of the helium atoms enters into the channels and compresses the liquid helium in the channel.

## IV. RESULTS

### A. Superfluid on bare channels

The observed superfluid signals for all studied diameters are shown in Fig. 2, where the temperature $T$ dependences of $\Delta F$ and $\Delta Q^{-1}$ due to the superfluid are plotted for a series of coverage. With decreasing $T$, $\Delta F$, which is proportional to the superfluid density $\rho_s$, begins to increase at the superfluid onset temperature $T_{on}$. $\Delta Q^{-1}$ has a peak associated with the superfluid transition at around $T_{on}$. For the 1.8 nm channel, the sharp resonant peaks in $\Delta F$ observed below $T_{on}$ are not an intrinsic behavior of this system because they are caused by a third-sound mode of the superfluid film on the grain surface, which resonates with the torsion frequency. [The large third-sound peaks are also observed in $\Delta Q^{-1}$. These peaks are 2 orders of magnitude larger than the dissipation peaks observed at $T_{on}$. For clarity, the third-sound peaks have been removed in Fig. 2(d).]

For each diameter, the shapes of $\Delta F$ for a series of $n$ are roughly similar to each other. Drastic changes in the behaviors of both $\Delta F$ and $\Delta Q^{-1}$ are found between the 2.8 and 2.2 nm channels. In the 4.7 and 2.8 nm channels, $\Delta F$ evolves slowly below $T_{on}$, which is in contrast to the sharp increase at $T_{on}$ for narrower channels. In addition, $\Delta F$ at $T=0$ for the 4.7 and 2.8 nm channels is 1 order of magnitude larger than that for narrower channels, if $\Delta F$ is normalized by $T_{on}$ and the surface area. $\Delta Q^{-1}$ for the 4.7 and 2.8 nm channels exhibits a large and broad peak below $T_{on}$, while, for narrower channels, very sharp peaks, which are more than 1 order of magnitude smaller than those for larger channels, are observed at $T_{on}$.

The coverage dependence of $T_{on}$ is displayed in Fig. 3. In the figure, the vertical lines indicate $n_f$, below which the adsorbed helium film forms a cylindrical tube on the wall of the channel. The superfluid film appears on the inert $^4$He film at $n_{on}$. On increasing $n$, the superfluid film becomes thick and $T_{on}$ increases roughly linearly with $n$. For a narrower channel, the superfluid appears closer to $n_f$. For the 4.7, 2.8, and 2.2 nm channels, $n_{on}$ is smaller than $n_f$, indicating that the helium film in the channel becomes superfluid. For the 1.8 nm channel, however, the superfluid appears at around $n_f$ and it is not clear whether the helium film in the channel becomes superfluid from these data.

For the 2.8 and 4.7 nm channels, a small substep is found in the two-dimensional isothermal compressibility obtained from our vapor pressure measurements.[19] The coverage at which the substep is found exactly agrees with $n_{on}$.

### B. Superfluid on substrates with $N_2$-filled channels

As the substrates are in powder form, the superfluid films are also formed on the outer surface of the substrate grains. Because such superfluid film contributes to the torsional oscillator signal, we cannot judge whether the detected signal originates from $^4$He in the channels or the films coating the substrate grains. To obtain clear evidence of the existence of the superfluid in the channels, we also performed the torsional oscillator measurements with the channels completely filled with $N_2$ atoms [Fig. 1(d)]. In this case, the superfluid signal originates only from the films coating the grain surfaces.

Figure 4 shows the temperature dependence of $\Delta F$ for the $N_2$-filled channels and that for bare substrates. For the 1.5 nm channel, the behaviors of $\Delta F$ for both bare and $N_2$-filled channels are very similar. On the other hand, for larger channels, the difference between the two cases is more evident. The sharp resonant peaks observed below $T_{on}$ for the 1.8 nm channel are due to the third-sound mode, not the intrinsic behavior.

For all diameters, the temperature dependences of $\Delta F$ for the $N_2$-filled cases are similar to each other, as shown in Fig. 5, when $T$ and $\Delta F$ are normalized by $T_{on}$ and $\Delta F$ $(T=0)$, respectively, proving that the superfluid signal in the $N_2$-filled cases comes only from the film on the grain surface.

The marked feature of the temperature dependence of $\Delta F$ in the $N_2$-filled cases is the discontinuous jump at $T_{on}$, which is peculiar to the KT transition. This is because the FSM grain size ($\sim$0.3 $\mu$m) is large enough that the grain surface can be regarded to have a flat geometry. In the KT theory, the amount of jump $\delta\rho_s$ of the superfluid density at $T_{on}$ is described by the universal relation $\delta\rho_s/T_{on}=2m^2k_B/\pi\hbar^2$, where $m$, $k_B$, and $\hbar$ are the mass of the $^4$He atom, Boltzmann's constant, and Planck's constant, respectively.[21] By comparing the observed jump with the KT universal relation, we obtain the surface area of the grains to be about 2% of the total surface area, which is in reasonable agreement with the value expected from the grain size ($\sim$1%).

The dependences of $T_{on}$ on $n$ for the bare substrate and for the $N_2$-filled channel are both displayed in Fig. 6. In the case

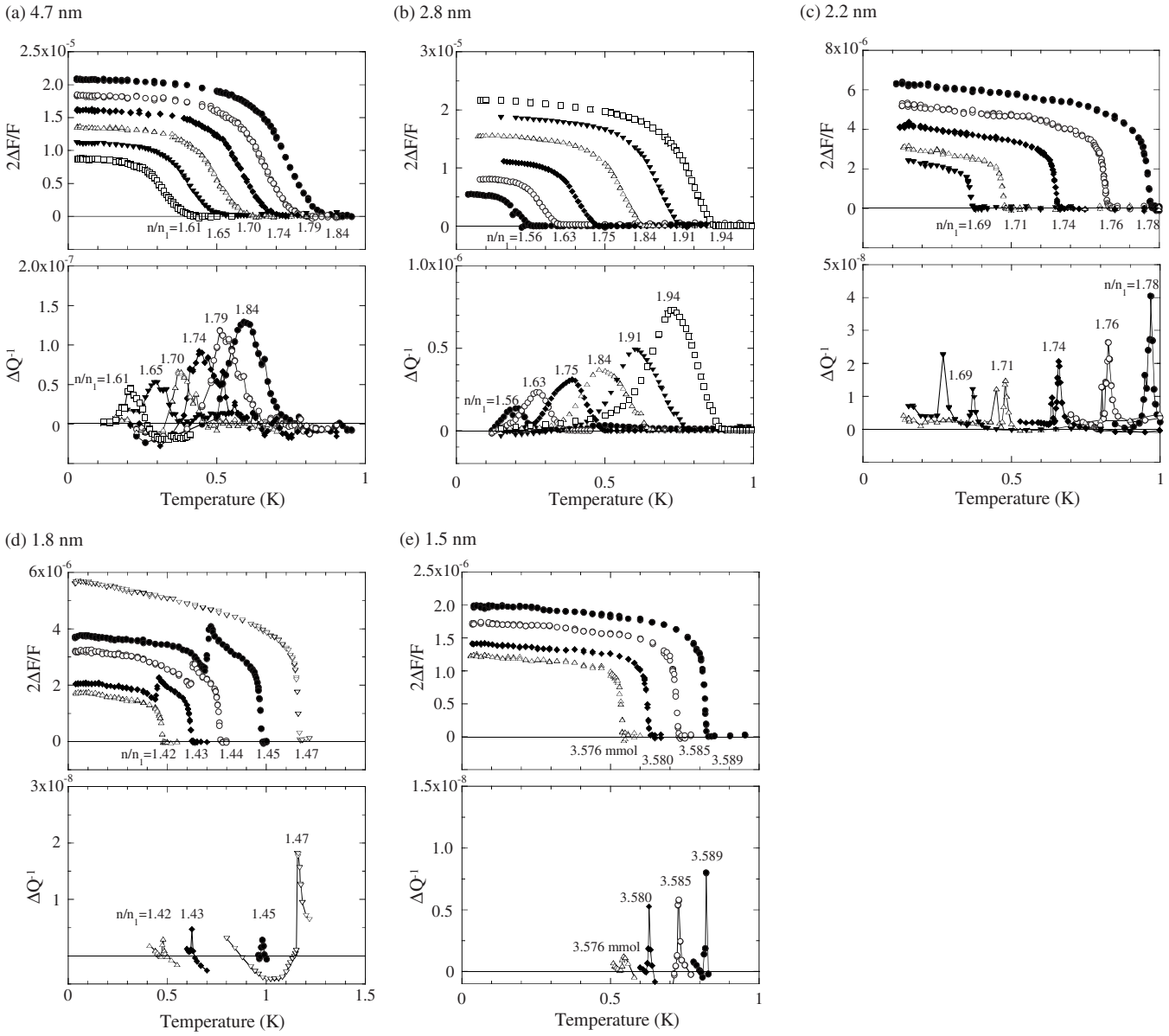


FIG. 2. Temperature dependence of frequency shift $2\Delta F/F$ and dissipation change $\Delta Q^{-1}$ of the torsional oscillators due to the superfluid transition for a series of coverage: (a) 4.7, (b) 2.8, (c) 2.2, (d) 1.8, and (e) 1.5 nm channels. For the 1.8 nm channel, the sharp resonant peaks observed slightly below $T_{on}$ are due to a third-sound mode excited in the superfluid film on the grain surface. Note that the scale of vertical axes of $2\Delta F/F$ and $\Delta Q^{-1}$ are more than 1 order different between the 2.8 and 2.2 nm channels.

of the $N_2$-filled channel, $n$ is shifted so that the superfluid onset coverage coincides with that of the bare substrate. For the 1.8 nm channel [Fig. 6(c)], the slope of $T_{on}$ against $n$ for the $N_2$-filled channel is 2.3 times steeper than that for the bare substrate. This suggests that the introduced $^4$He atoms are adsorbed both into the channels and onto the grain surface at a ratio of 1.3:1. This value is consistent with 1.7:1 obtained by the vapor pressure measurements.[19] $^4$He in the channel is gradually compressed as more $^4$He atoms are introduced, indicating that a part of $^4$He in the channel is rather soft and therefore liquid. On the other hand, in the 1.5 nm channel [Fig. 6(d)], the $n$ dependences of $T_{on}$ in the two cases completely overlap, suggesting that $^4$He in the channel is difficult to compress and hence solid.

## V. DISCUSSION

### A. Comparison of superfluid properties for bare channels and for $N_2$-filled channels

In Fig. 7, the frequency shifts for the bare channels and for the $N_2$-filled channels are compared. For the $N_2$-filled channels, the coverage with the closest $T_{on}$ to that of the bare substrates is selected, and the vertical and horizontal axes are multiplied with the same value (almost unity) so that $T_{on}$ coincides with that of the bare substrate. The comparison of the data with the same $T_{on}$ in this manner is based on the following reason. In the torsional oscillator experiment, in general, the superfluid can be detected only when the superfluid film is macroscopically connected. In our cases, the

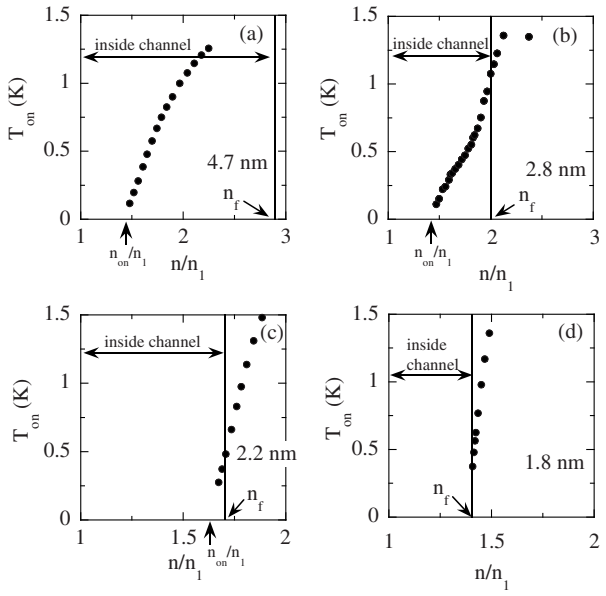


FIG. 3. Superfluid onset temperature for (a) 4.7, (b) 2.8, (c) 2.2, and (d) 1.8 nm channels as a function of coverage. $n_f$ is the full pore coverage (Ref. 19). Below $n_f$, the adsorbed $^4$He film forms a cylindrical tube in the channel.

superfluids in the channels are connected with each other through the films on the grain surface. This causes the problem that, when the film on the grain surface is a normal fluid, the isolated superfluid in the channel is not connected macroscopically and is never detected.[22] To obtain a clear picture, we consider two cases: $T_{on}^{channel} > T_{on}^{grain}$ and $T_{on}^{channel} < T_{on}^{grain}$, where $T_{on}^{channel}$ is the transition temperature of the liquid in the channel and $T_{on}^{grain}$ is that of the film on the grain surface. If $T_{on}^{channel} > T_{on}^{grain}$, the superfluid in the channel is isolated when the film on the grain surface is normal, and no superfluid signal is detected in spite of the existence of the superfluid in the channel [Fig. 8(a)]. The superfluid signal is detected only at $T < T_{on}^{grain}$, and therefore the observed $T_{on}$ is $T_{on}^{grain}$. On the other hand, if $T_{on}^{channel} < T_{on}^{grain}$, the superfluid signal from the grain surface is detected below $T_{on}^{grain}$, and the additional superfluid signal from the channel is observed below $T_{on}^{channel}$ [Fig. 8(b)]. Thus, in any case, the observed $T_{on}$ is always $T_{on}^{grain}$. Consequently, if we compare the films with the same $T_{on}$ as in Fig. 7 (thus, the same thickness of the film on the grain surface), the same amount of $\Delta F$ is expected if $^4$He in the channel does not become superfluid.

For the 1.5 nm channel, $\Delta F$ in both cases shows the same temperature dependence as illustrated in Fig. 7(d). Moreover, $T_{on}$ has the same coverage dependence in both cases [Fig. 6(d)]. These two findings prove that the detected superfluid signal for the bare channel comes only from the film coating the grain surface, and therefore $^4$He in the channel is not superfluid.

For the other channel diameters [Figs. 7(a)–7(c)], a clear difference is found between the bare channel and the $N_2$-filled channel, proving that $^4$He in the channel is superfluid. In the case of the bare channel, the additional superfluid signal originating from $^4$He in the channel is superim-

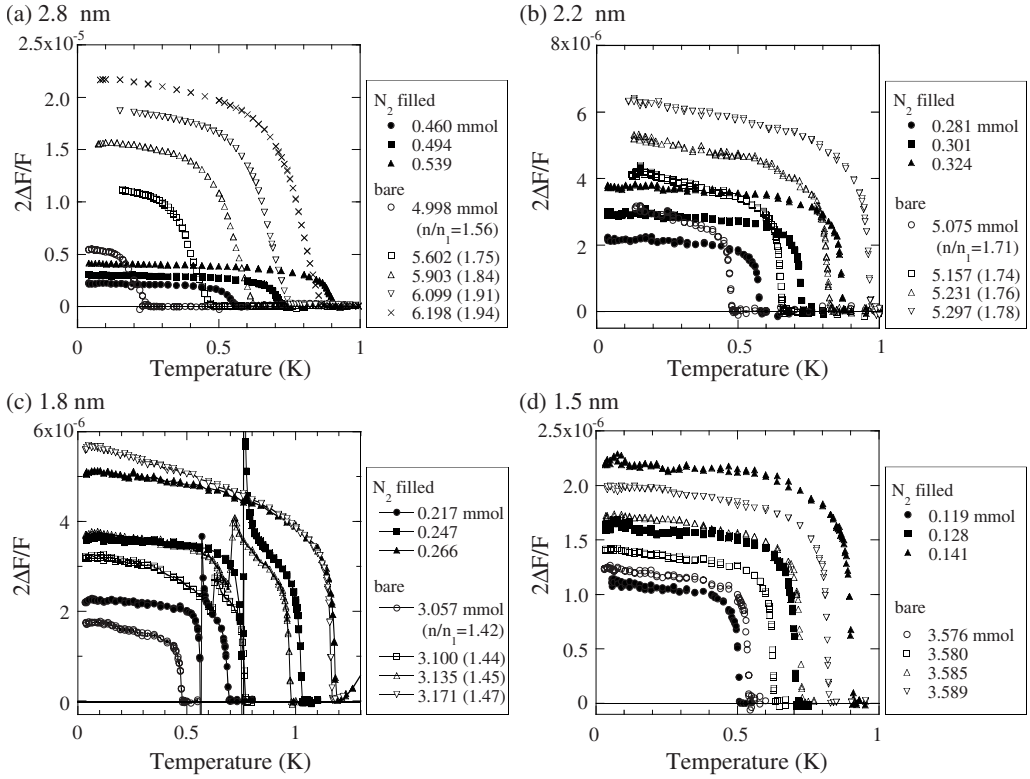


FIG. 4. $2\Delta F/F$ for the $N_2$-filled channels and the bare channels: (a) 2.8, (b) 2.2, (c) 1.8, and (d) 1.5 nm channels. For the 1.8 nm channel, the sharp resonant peaks are due to the third-sound mode excited in the film on the grain surface.

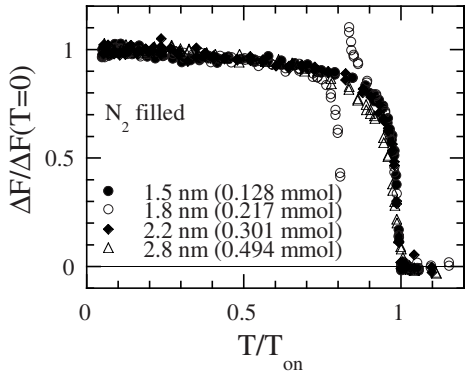


FIG. 5. Normalized frequency shift $\Delta F/\Delta F\,(T=0)$ as a function of $T/T_{on}$ for the $N_2$-filled channels with various diameters. The sharp resonant peak at $T/T_{on}=0.8$ observed for the 1.8 nm channel is due to the third-sound resonance.

posed on the superfluid signal from the film coating the grain surface.

The possibility that the observed difference in Figs. 7(a)–7(c) (particularly for the 1.8 nm channel) could be caused by a change in the available area of the grain surface as a result of $N_2$ adsorption is excluded because of the result for the 1.5 nm channel. For the 1.5 nm channel, the same temperature dependence of $\Delta F$ [Fig. 7(d)] and the same $n$ dependence of $T_{on}$ [Fig. 6(d)] prove that the adsorption of $N_2$ does not change the area of the grain surface.

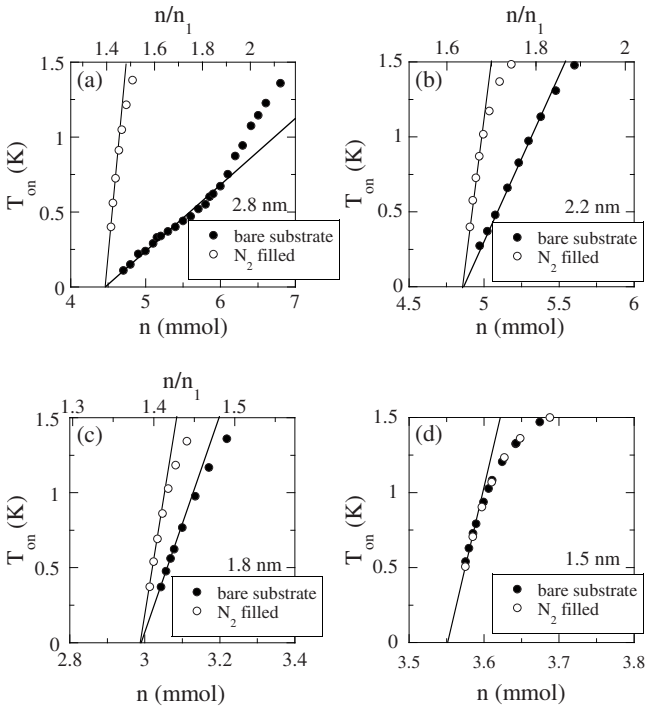


FIG. 6. Coverage dependence of the superfluid onset temperature for the bare channel (●) and the $N_2$-filled channel (○): (a) 2.8, (b) 2.2, (c) 1.8, and (d) 1.5 nm channels. In the case of the $N_2$-filled channel, $n$ is shifted so that the superfluid onset coverage coincides with that of the bare channel.

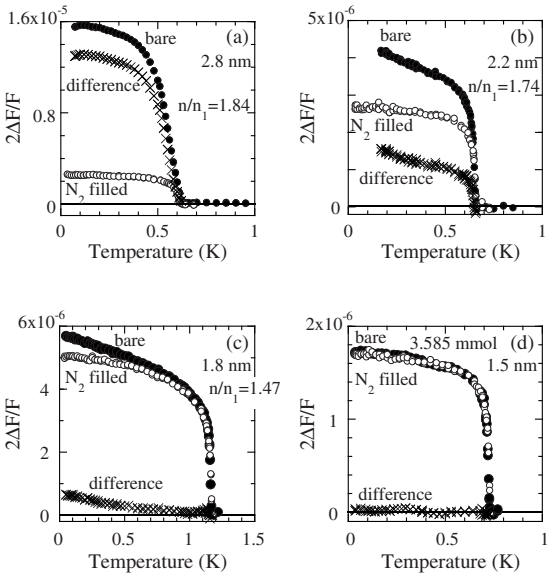


FIG. 7. $2\Delta F/F$ for the bare channel (●) and for the $N_2$-filled channel (○) with the same $T_{on}$ (see text). The difference between the two (×) is also shown: (a) 2.8, (b) 2.2, (c) 1.8, and (d) 1.5 nm channels.

### B. Channel-diameter dependence of superfluid properties

The KT transition in 2D systems occurs when the vortex pairs of infinite separation are unbound, and these unbound vortices destroy the phase coherence. In the cylindrical geometry with $d>a_0$, vortex-antivortex confinement occurs along the channel axis because the energy required to separate two vortices grows linearly to the axial separation. Consequently, the unbound vortices separated by less than $\pi d/2$ destroy the phase coherence and determine the transition temperature.[11–13] This finite-size KT transition with the system size of $\pi d/2$ predicts the continuous evolution of the superfluid density below $T_{on}$ and explains the observed superfluid properties in porous glass with channel diameter larger than 5 nm.[15]

In Fig. 9, we show the frequency shifts for various diameters, which are obtained as the difference between the frequency shift for the bare substrate and that for the $N_2$-filled one for a coverage shown in Fig. 7. In Fig. 9, the result for

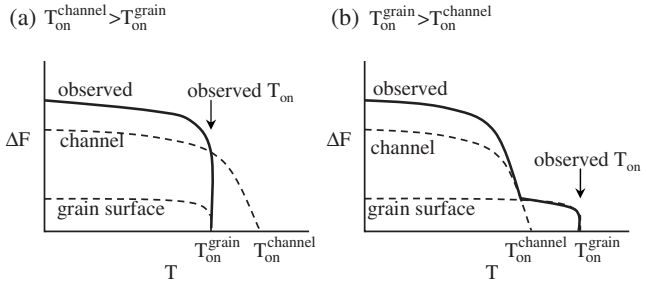


FIG. 8. Schematic illustration of the expected frequency shifts for (a) $T_{on}^{channel}>T_{on}^{grain}$ and (b) $T_{on}^{grain}>T_{on}^{channel}$. The dashed lines represent the temperature dependence of the superfluid density for each case.

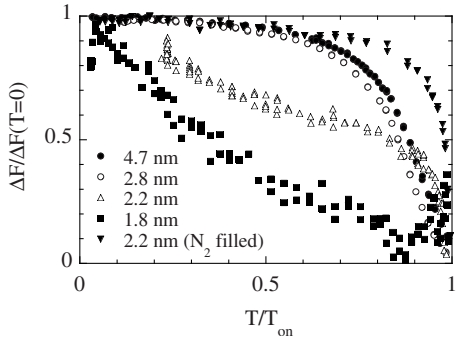


FIG. 9. The difference between the frequency shift for the bare channel and that for the $N_2$-filled one for a coverage shown in Fig. 7. The vertical axis is normalized by the frequency shift at the zero temperature limit. The result for the $N_2$-filled 2.2 nm channel is shown as a typical representative of the KT transition.

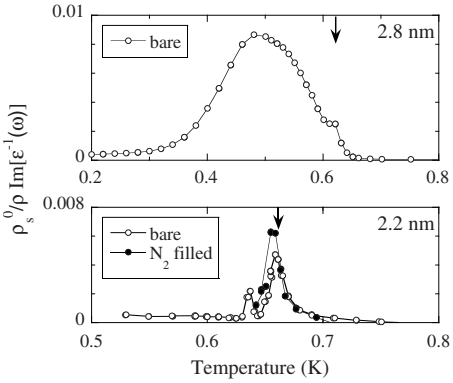


FIG. 10. The normalized dissipation for the bare 2.8 and 2.2 nm channels. The arrows indicate $T_{on}$. In the case of the 2.8 nm channel, the small shoulder observed at $T_{on}$ is due to the KT transition of the film coating the grain surface. In the case of the 2.2 nm channel, the result for the $N_2$-filled channel is also shown.

the $N_2$-filled 2.2 nm channel is included as a typical representative of the KT transition. In the 4.7 and 2.8 nm channels, below $T_{on}$, the superfluid density evolves slowly compared with the KT transition. A similar behavior was observed for the $^4$He film adsorbed in the porous glass 5.0 nm in diameter[15] and is considered to be characteristic of the finite-size KT transition. In contrast, the behavior of the superfluid density changes drastically for the 2.2 and 1.8 nm channels. In these channels, the superfluid density evolves very slowly and is greatly suppressed even at $T<0.5T_{on}$ compared with the 4.7 and 2.8 nm channels.

The drastic change in the behavior of $\Delta Q^{-1}$ is also found between the 2.2 and 2.8 nm channels, as seen in Fig. 2. For the 4.7 and 2.8 nm channels, $\Delta Q^{-1}$ shows a large and broad peak below $T_{on}$, while $\Delta Q^{-1}$ for the 2.2 and 1.8 nm channels has a sharp peak at $T_{on}$. From the (finite-size) KT theory, the dissipation peak appears due to the diffusive motion of vortices driven by the oscillating superflow induced by the torsional motion of the cell. To compare the dissipation peak quantitatively, we calculate the normalized dissipation used in the dynamic KT theory,[23] which is defined by

$$\frac{\rho_s^0}{\rho}\,\mathrm{Im}[\varepsilon^{-1}(\omega)] = \frac{F}{2(1-\chi)(n-n_{on})|\partial F/\partial n|_n}\Delta Q^{-1}, \quad (1)$$

where $\rho_s^0$ is the bare superfluid density and $\varepsilon(\omega)$ is the dielectric function defined in the dynamical KT theory. The normalized dissipation for the 2.2 and 2.8 nm channels is plotted in Fig. 10. The integrated area below the normalized dissipation curve in Fig. 10 gives a measure of the dissipation associated with the diffusive motion of vortices. The areas for the 4.7 and 2.8 nm channels are comparable to that for a Mylar substrate (the typical KT transition)[24] when the films with the same $T_{on}$ are compared, but they are 2 orders of magnitude larger than those for the 2.2 and 1.8 nm channels. This fact is an additional evidence that the vortex mechanism plays an important role in the transition in the 2.8 and 4.7 nm channels.

The dissipation in the 2.2 nm channel has double peaks, as illustrated in Fig. 10, for all studied coverages. The peak at the higher temperature is attributable to the superfluid transition of the film coating the grain surface because it appears at the same temperature as in the $N_2$-filled case with a similar magnitude. The lower peak originates from the superfluid in the channel. In the 1.8 nm channel, the peak from $^4$He in the channel is not found. The small dissipation in the 1.8 and 2.2 nm channels indicates that the vortex mechanism is irrelevant.

In the 2.2 nm channel, the effective diameter is inferred to be about 1.0 nm, taking into consideration the approximately two layers of inert $^4$He. This effective diameter is small enough for the break down of the finite-size KT transition ($d \leqslant a_0 = 2.5 \pm 1.2$ nm).

### C. Superfluid properties in 1.8 and 2.2 nm channels

The most interesting question is how one dimensionality influences the superfluidity. In the previous section, we described that the superfluid is strongly suppressed in the 1.8 and 2.2 nm channels. For these channels, the finite-size KT transition mechanism breaks down, and the superfluid properties seem to be affected by the one dimensionality. In this section, we discuss the superfluid properties for these channels referring to the existing heat capacity data.[3]

In Fig. 11, the coverage dependence of $T_{on}$ for the 1.8 nm channel is shown with the isotherms of the molar heat capacities of $^4$He and $^3$He, which were previously obtained by our group.[3] At $n<1.15n_1$, the film is considered to be solid because the isotherms of $^4$He show the same coverage dependence as those of $^3$He. At $n>1.15n_1$, on the other hand, the isotherms of $^4$He show a quantitatively different coverage dependence from those of $^3$He. This strongly suggests that the quantum fluid film (i.e., Bose fluid for $^4$He and Fermi fluid for $^3$He) appears at $1.15n_1$. In this quantum fluid region ($1.15n_1<n<n_f$), the heat capacity of $^4$He film is proportional to the temperature, which is attributed to the 1D phonons propagating along the channel axis.[3,10] In the channel, only the phonons along the channel axis are excited because the phonons propagating in the azimuthal direction have discrete energy levels with an energy separation of the order of kelvin.

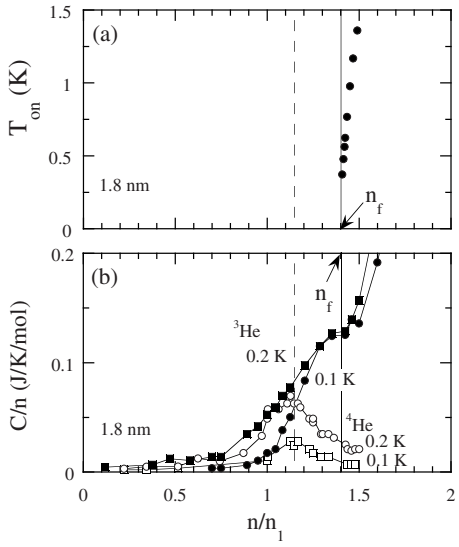


FIG. 11. (a) Coverage dependence of $T_{on}$ and (b) isotherms of molar heat capacities of $^4$He and $^3$He for the 1.8 nm channel (Ref. 3). The isotherms of $^4$He and $^3$He show qualitatively different coverage dependences at $n > 1.15n_1$, indicating that the film is a quantum liquid in this coverage regime. The dashed line indicates $1.15n_1$.

In this Bose fluid region ($1.15n_1 < n < n_f$), we do not observe the superfluid, as shown in Fig. 11. However, because the isolated superfluid in the channel is never detected by the torsional oscillator when the film on the grain surface is a normal fluid, as discussed above, there is a possibility that the film in the channel is superfluid in this coverage region but not detected because of the normal fluid on the grain surface. Other techniques to detect the isolated superfluid in the channel will yield important information about the relationship between the superfluidity and the 1D phonons.

Above $n_f$, we observe the superfluid for both the 1.8 and 2.2 nm channels. In this region, the state of $^4$He in the channel is not a film but liquid which fills the channel. The effective diameter of the liquid is approximately 0.6 and 1.0 nm for the 1.8 and 2.2 nm channels, respectively, taking into account two inert $^4$He layers. In this region, the thermal excitation is also expected to be that of the 1D phonon, which gives rise to the normal density $(\pi k_B^2/3\hbar c^3)T^2$ at low temperatures. The observed frequency shift, however, shows a rather linear temperature dependence at low temperatures (Fig. 9) and is greatly suppressed compared with the phonon contribution. This strong suppression of superfluid density seems to be relevant to the strong phase fluctuation peculiar to low-dimensional systems.

Above $n_f$, the phase of the order parameter in the cross section of the channel seems to align uniformly because the effective diameter is comparable to the coherence length of bulk $^4$He superfluid ($\sim$0.3 nm). Therefore, the system is regarded as a 1D system as far as the phase fluctuation is concerned. In the 1D system, the phase fluctuation of the order parameter is significant and it destroys the long-range order. The correlation function decays exponentially at a long distance and the superfluid should not be observed. One possible explanation for our observation of the superfluid in such narrow channels is that the finite length of the channel ($\sim$0.3 $\mu$m) would give rise to a finite transition temperature. Theoretical calculations demonstrated that the 1D Bose-Einstein condensation can take place in an ideal Bose gas with a finite number of particles.[25,26] These calculations, however, treat a noninteracting system. Another possibility is that the three-dimensional coupling of the superfluids in the channels through the superfluid films coating the grain surface suppresses the phase fluctuation. However, we have no theory that can explain the existence of the superfluid in such narrow channels at present, and such a theory should be developed.

## VI. CONCLUSIONS

We have conducted systematic studies of the properties of superfluid $^4$He adsorbed in nanometer-size channels of various diameters ranging from 1.5 to 4.7 nm, using torsional oscillators. Clear evidence was obtained that $^4$He becomes superfluid in channels with diameter larger than 1.8 nm. In channels larger than 2.8 nm, the superfluid transition is well explained by the finite-size Kosterlitz-Thouless transition. In contrast, the superfluid in channels narrower than 2.2 nm, where the channel size is smaller than the vortex core diameter, shows a strong suppression of the superfluid density and a small dissipation at the transition. These features strongly suggest that the vortex mechanism plays no role in the transition and that the superfluid properties are affected by the one dimensionality.

## ACKNOWLEDGMENTS

This work was partly supported by Grants-in-Aid for Scientific Research on Priority Areas (Grant Nos. 17071006 and 17204029) from the Ministry of Education, Culture, Sports, Science and Technology of Japan.

*hikegami@riken.jp

[1] J. M. Kosterlitz and D. J. Thouless, J. Phys. C **6**, 1181 (1973).
[2] D. J. Bishop and J. D. Reppy, Phys. Rev. Lett. **40**, 1727 (1978).
[3] N. Wada, J. Taniguchi, H. Ikegami, S. Inagaki, and Y. Fukushima, Phys. Rev. Lett. **86**, 4322 (2001).
[4] J. Taniguchi, T. Okuno, H. Ikegami, and N. Wada, J. Low Temp. Phys. **126**, 259 (2002).
[5] M. W. Cole and E. S. Hernández, Phys. Rev. B **65**, 092501 (2002).
[6] G. Stan and M. W. Cole, Surf. Sci. **395**, 280 (1998).
[7] Y. Yamato, H. Ikegami, T. Okuno, J. Taniguchi, and N. Wada, Physica B **329-333**, 284 (2003).
[8] H. Ikegami, Y. Yamato, T. Okuno, J. Taniguchi, and N. Wada, J. Low Temp. Phys. **138**, 171 (2005).

[9] H.-C. Chu and G. A. Williams, J. Low Temp. Phys. **138**, 343 (2005).
[10] J. Taniguchi, H. Ikegami, and N. Wada, Physica B **329-333**, 274 (2003).
[11] T. Minoguchi and Y. Nagaoka, Prog. Theor. Phys. **80**, 397 (1988).
[12] J. Machta and R. A. Guyer, Phys. Rev. Lett. **60**, 2054 (1988).
[13] F. Gallet and G. A. Williams, Phys. Rev. B **39**, 4673 (1989).
[14] V. Kotsubo and G. A. Williams, Phys. Rev. Lett. **53**, 691 (1984).
[15] K. Shirahama, M. Kubota, S. Ogawa, N. Wada, and T. Watanabe, Phys. Rev. Lett. **64**, 1541 (1990).
[16] S. Inagaki, Y. Fukushima, and K. Kuroda, J. Chem. Soc., Chem. Commun. **1993**, 680.
[17] S. Inagaki, A. Koiwai, N. Suzuki, Y. Fukushima, and K. Kuroda, Bull. Chem. Soc. Jpn. **69**, 1449 (1996).
[18] S. Inagaki, Y. Yamada, Y. Fukushima, and K. Kuroda, Stud. Surf. Sci. Catal. **92**, 143 (1994).
[19] H. Ikegami, T. Okuno, Y. Yamato, J. Taniguchi, N. Wada, S. Inagaki, and Y. Fukushima, Phys. Rev. B **68**, 092501 (2003).
[20] N. Wada, J. Taniguchi, T. Matsushita, R. Toda, Y. Matsushita, H. Ikegami, M. Hieda, A. Yamaguchi, and H. Ishimoto, J. Phys. Chem. Solids **66**, 1512 (2005).
[21] D. R. Nelson and J. M. Kosterlitz, Phys. Rev. Lett. **39**, 1201 (1977).
[22] Isolated superfluid is completely locked to the motion of a torsional oscillator, resulting in no change in the inertia of the oscillator.
[23] V. Ambegaokar, B. I. Halperin, D. R. Nelson, and E. D. Siggia, Phys. Rev. B **21**, 1806 (1980).
[24] H. Yano, T. Jocha, and N. Wada, Phys. Rev. B **60**, 543 (1999).
[25] W. Ketterle and N. J. van Druten, Phys. Rev. A **54**, 656 (1996).
[26] V. A. Alekseev, J. Exp. Theor. Phys. **94**, 1091 (2002).